Breakage functions of particles of four different materials subjected to uniaxial compression

Singh, Dharminder; McGlinchey, Don; Crapper, Martin

Published in:
Particulate Science And Technology

DOI:
10.1080/02726351.2016.1185201

Publication date:
2016

Document Version
Author accepted manuscript

Breakage functions of particles of four different materials subjected to uniaxial compression

Dharminder Singh[1], Don McGlinchey[1] & Martin Crapper[2]

1. School of Engineering and Built Environment, Glasgow Caledonian University, Glasgow G51 1SG, United Kingdom
2. School of Engineering, The University of Edinburgh, Edinburgh EH9 3JL, United Kingdom

Abstract

Particle breakage is a common problem in the conveying and handling of particulate solids. The phenomenon of particle breakage has been studied by experiments by a number of researchers in order to describe the process of breakage by mathematical functions. The development of comminution functions that can suitably describe the breakage behaviour of granular materials can lead to a significant improvement in the design and efficiency of particulate solids handling equipment. The present study focuses on developing the strength distribution and the breakage functions of particles of four different materials subjected to uniaxial compressive loading. Single particles were compressed until fracture in order to determine their strength distribution and the fragments were investigated to determine their size distribution. The parameters of logistic function and breakage function were obtained by curve-fitting of the functions to the strength distribution and size distribution of the fragments respectively. These functions were then implemented in the BGU-DEM code which was used to carry out Discrete Element Method (DEM) simulations on single particle breakage by compression. The simulations produced a similar mass distribution of fragments to the breakage function obtained from the experimental data.

Keywords: Particle breakage, DEM, Strength distribution, Breakage function, Compression

Introduction

In the recent years, research on particle breakage has attracted a lot of interest in the particulate solids handling industry, where it is a common issue. Particle breakage can be desirable or undesirable depending upon the application, i.e. it is desirable in rock crushing/milling applications whereas it is undesirable in the chemical and pharmaceutical industries during the handling and transportation of granules or agglomerates as it degrades the quality of the product. In both cases, it is essential to study the process of particle breakage in order to improve the efficiency of particulate solids handling equipment.

A number of researchers have investigated the phenomenon of particle breakage by using mathematical comminution functions. Some researchers have used compression tests (Subero-Couroyer et al. 2003; Pitchumani et al. 2004; Rozenblat et al. 2011) whereas others have used impact tests (Vogel and Peukert 2002; Wu et al. 2004) to determine these comminution functions. Kalman et al. (2009) presented a new method to implement five comminution functions into Discrete Element Method (DEM) simulations to simulate the process of particle breakage: strength distribution, selection, breakage, equivalence and fatigue functions. The present study focuses on determining the strength distribution and breakage functions of four different materials by using uniaxial compression tests. These functions are important because the strength distribution function determines whether a particle will break under an applied force whilst the breakage function determines the size distribution of the fragments produced as a result of particle breakage.

Strength distribution function

In the compression tests, as discussed in this work, a single particle was subjected to uniaxial compression between two platens until fracture, and the force required to break the particle was recorded as the crushing force. Due to the presence of pores and existing cracks, the

strength of individual particles is not identical (Subero-Couroyer et al. 2003), so a large number of particles was tested in order to determine a statistically reliable strength distribution which can then be described by a statistical function. Table 1 shows the number of particles tested and the statistical functions used by some previous researchers. In this table, P is the probability of particle breakage, F is the crushing force and, a and b are empirical model parameters. The logistic function was used to describe the strength distribution in the present study because it gives a good fit to the experimental data and is mathematically simple (Rozenblat et al. 2011).

Breakage function

According to Kalman et al. (2009), the cumulative mass or volumetric function B can be expressed by:

$$B = \left(\frac{d_f}{d_{max}}\right)^c \tag{4}$$

where, d_f is the fragment size, d_{max} is the largest particle size in the population of fragments and c is an empirical parameter. This function is based on Vogel and Peukert's (2002) breakage function.

Objectives

The objectives of our research were:

i. to apply the logistic function and the breakage function to describe the particle strength distribution and fragment size distribution respectively, and so to determine empirical parameters for four specific particulate materials, namely mustard seeds, black peppercorns, unrefined cane sugar and cake decorations; and

ii. to implement these in a DEM code to simulate breakage of single particles.

BGU-DEM (Brosh and Levy 2010; Brosh et al. 2011b) was chosen for simulations as it includes the breakage model of Kalman et al (2009).The BGU-DEM code was linked to ANSYS FLUENT 13.0. Initially the particles are assigned a strength from the strength distribution found from the experiments. The particle breaks once the force acting on the particle exceeds its strength and fragments are created in place of the mother particle. The sizes of the daughter particles are determined from the breakage function.

Experiments

In order to investigate particle breakage, experiments were conducted using a TA XTPlus Texture Analyser (Stable Micro Systems Ltd, Godalming, UK) which is shown in Fig. 1. It is capable of measuring physical characteristics of materials such as breakage strength, hardness, cohesion, adhesion, stiffness, etc. by compression, tension, bending or shearing tests. It is equipped with a load cell capable of measuring loads up to 30 kg (294.3 N) with a resolution of 0.1 g. The Texture Analyser is connected to a computer system which is used for control and to record the force and displacement as a function of time. A cylindrical probe of 6 mm diameter was used to compress each particle at a constant rate of 1 mm/s. As the probe moves downwards, the software records the force and displacement values, and generates a graph which can be used to determine the breakage force. When the pre-set maximum value of the force is reached the probe retracts to its original position.

The first set of experiments for finding the strength distribution function were conducted using 100 particles each of the four different materials. The particle size was measured with a Vernier calliper before testing each particle. The particle was then placed on the platform and Texture Component 32 software was used to control the compression test. Table 2 lists the materials used and their sizes, whilst Fig. 2 illustrates the particles used. All the particles tested were approximately spherical apart from the unrefined cane sugar particles which were

roughly cuboidal. It was found that the mustard particles do not break into fragments, but are grossly deformed.

A second set of experiments was conducted to study the size distribution of the fragments resulting from particle breakage. These involved testing 10 particles of each material except the mustard seeds, which did not fragment. For these experiments, each test was stopped after the particle broke. The fragments formed were then carefully collected on glass slides, to be examined by optical microscopy using a Leica DM500 microscope.

Results and Discussion

A typical force-displacement curve obtained for a black peppercorn particle of size 4.14 mm is shown in Fig. 3. The graph has been divided into four regions. In Region A, the probe is moving towards the particle so the force is zero. When the probe comes in contact with the particle at the start of Region B, the force starts to rise as the particle is being compressed. The force continues to rise until the particle breaks at which point the force drops suddenly. The probe continues to compress the fragments of the particle. These fragments get rearranged under the probe and get broken into smaller fragments, the force response to which appears as peaks in Region C. When the fragments are completely compressed, the force begins to rise at a higher rate as can be seen in Region D after which the probe returns to its original position and it is ready to test the next particle. It should be noted that for the second set of experiments, in order to investigate the fragments formed after primary breakage, the test was stopped at the end of Region B.

The region B and region C in Fig. 3 appear to be similar to force-displacement graph obtained by Khanal et al (2005) however towards the end of Region C, the force response is higher on their graph. This could be due to the larger size and the higher strength of the particles tested by them.

Strength Distribution Function

We have expressed the strength of the particles in terms of crushing force, which was obtained from the peak in the Region B of Fig. 3. The crushing force was recorded for all the particles and the results are shown in Table 3. The table shows the maximum, minimum, mean, median and standard deviation of crushing force found for material. As mentioned earlier, it can be seen that there is wide variation in the strength for each of the materials.

As mentioned previously, in order to describe the particle strength distribution, a statistical function is needed. Rozenblat et al. (2011) reported that all the functions mentioned in Table 1 can describe the strength distribution satisfactorily but they chose the logistic function (Eq. (3)) for its mathematical simplicity. It does not consist of any complex mathematical expressions such as an exponent function (in Weibull) or an error function (in lognormal). By the same reasoning, the logistic model was chosen to represent the strength distribution of the particles in this study. The parameters also have statistical meanings: parameter a is the median, and parameter b is the dispersion of the distribution. If b is larger, the distribution would be narrower and if it is smaller, the distribution would be wider. The logistic function was then fitted to the experimental data using the Least Mean Squares method. The values of parameters a and b and coefficient of determination R^2 were determined and are shown in Table 4. It can be seen that the values of parameter a are quite close to the median crushing force values determined from the experiments. Fig. 4 shows the logistic function fit for all the materials, from which it is clear that the logistic function describes the experimental data well.

Breakage function

This section describes the size distributions of fragments formed from the particles and how the breakage functions were determined. It was found that peppercorn particles fragmented

into 3 to 5 fragments. Cake decorations were found to break into 8 to 111 fragments and unrefined cane sugar into 21 to 65 fragments out of which 3 to 10 fragments accounted for 90% of the mass of the parent particle, the remaining fragments being very small.

The mass of a fragment relative to the parent particle can be determined using the following relation:

$$m_{rel} = \frac{m_f}{m_T} \tag{5}$$

where, m_f is the mass of the fragment and m_T is the total mass of the fragments, which is also equal to the mass of the parent particle.

The breakage functions determined in this study were subsequently used in BGU-DEM code which can simulate only spherical fragments after breakage (Brosh et al. 2011a). Thus, for a fragment of size d_f and the parent size d_p (assuming constant density), Eq. (5) was re-written as:

$$m_{rel} = \frac{V_f \rho}{V_p \rho} = \frac{\frac{1}{6}\pi d_f^3}{\frac{1}{6}\pi d_p^3} = \left(\frac{d_f}{d_p}\right)^3 \tag{6}$$

As the actual fragments are non-spherical, the sum total of relative mass of all the fragments found by Eq. (6) will be greater than unity. Therefore, the relative mass of the fragments was normalised dividing it by the sum of the relative mass of all the fragments as shown in Eq. (7).

$$m_{norm} = \frac{m_{rel}}{\sum m_{rel}} \tag{7}$$

The fragment sizes measured by microscope (Feret diameter) were used to calculate the relative mass of fragments using Eq. 6 which was then normalised using Eq. 7. Fig. 5 shows the typical size distributions of fragments obtained using this method for a particle of each material. The horizontal axis shows the cumulative normalised mass while the vertical axis shows the cumulative ratio of number of fragments to total fragments. From the 5 fragments

of the peppercorn particle shown here, 4 were found to be nearly the same size and 1 a smaller size whereas the cake decoration and the unrefined cane sugar particles produced a large variety of fragment sizes. From a total of 111 fragments of the cake decoration particle, only 6 fragments make up the 90% of the mass of the parent particle. The remaining 10 % of the mass is split into the rest of the 105 fragments. A similar pattern can be seen for the unrefined cane sugar particle where the mass of just 3 fragments (from a total of 28) is equal to 90% of the parent particle and the remaining 25 fragments form just 10% of the mass of parent particle.

The breakage function (Eq. (4)) was then fitted to the cumulative normalised mass distribution of the fragments using the Least Mean Squares method and the parameter *c* was determined. The curve fitting is shown in Fig. 6. The graphs show cumulative normalised mass on the vertical axis and the particle size on the horizontal axis. It can be seen that there is a good agreement between the breakage function and the experimental data. Table 5 shows the values of parameter *c* obtained from the curve fitting procedure.

Simulation of particle breakage using DEM

A cylindrical domain was created as shown in Fig. 7. The bottom surface was modelled as a stationary wall on which the particle (as a sphere) was placed. A moving wall was created above the particle which moves downwards to compress the particle. The strength distribution and breakage functions were implemented in DEM according to the procedure described by Kalman et al (2009). The DEM code has been used in the past to simulate breakage by impact (Brosh et al. 2011b; Brosh et al. 2014) in which the impact velocity needed to be converted to an equivalent force. Therefore, the code was modified to simulate compression based breakage by making the equivalent force to be equal to the magnitude of

the force acting on the particle. A similar breakage mechanism has also been used recently by Cleary and Sinnott (2015) to simulate particle breakage in compression crushers.

The contact force F acting on the particle was modelled by a spring-dashpot model which is calculated by:

$$F = k\delta^{1.5} - Cv \tag{8}$$

where, δ is the displacement of the particle (due to compression), C is the damping coefficient, v is the relative velocity of particle to the wall, k is the spring stiffness between the particle and the wall which is calculated as:

$$k = \frac{4}{3}\left[\frac{\sqrt{r}}{(1-\upsilon_p^2)/E_p + (1-\upsilon_w^2)/E_w}\right] \tag{9}$$

where, r is the radius of the particle, υ is the Poisson's ratio and E is the Young's Modulus. The subscripts p and w stand for particle and wall respectively. The particle and wall properties used in the simulations are shown in Table 6. The Young's Modulus of the particles was determined by single particle compression experiments based on the method used by Couroyer et al. (2000). Single particles were loaded and unloaded twice in the force range of 2-5 N. The Young's Modulus of the particles was obtained from the second unloading curve based on the Hertz force-displacement relation.

The particle breaks when the force acting on it exceeds its strength, and daughter particles are created in its place based on the breakage function. Fig. 8 shows an example of how the fragments are formed after breakage for each kind of particle. The particles are coloured according to their size. The peppercorn particle fragmented into 2, the unrefined cane sugar particle into 12 and the cake decoration particle into 5 daughter particles.

Fig. 9 shows the comparison of the fragment size distribution of five particles of each kind obtained after breakage and the breakage function used in the DEM code. The parent particles were of different sizes, so the mass distribution is shown as a function of the ratio of

fragment size to the size of the largest fragment. It can be seen the mass distribution of the fragments of all the materials closely resembles the distribution expected by the breakage function obtained from the experimental data which demonstrates the suitability of the DEM code and the functions used to simulate the particle breakage.

Predictive simulation

The DEM code was then used for predicting breakage in the bulk crushing of peppercorns. The results were compared to experimental data for these tests. In the experiments, about 300 particles were taken in a cylindrical container with an internal diameter of 40 mm. The particle bed was compressed by 5 mm at a rate of 1 mm/min using an Instron compression machine. The size distribution of the particles was measured using sieves before and after the compression experiment. The schematic of the experimental set up is shown in Fig. 10.

For the simulations, a cylindrical domain of 40 mm diameter and 40 mm height was created. Then 300 particles were dropped into the domain from the top. The particle size range was from 3.34 mm to 5.15 mm. This gave a similar size distribution as the experiments as shown in Fig. 11. The particles settled in the bottom part of the cylinder under gravity and form a particle bed. The coefficient of restitution between the particles was 0.3 and between the particles and the walls was 0.5. A moving wall then starts to compress the particle bed. The simulation was stopped after a compression of 5 mm after first contact. The time-step for the simulation was 2 μs. Fig. 12 shows the visualisation of the particle assembly before compression and at the end of 5 mm compression. The broken particles are shown in black whereas the particles in white are the unbroken particles. It was found that after a compression of 5 mm, 43 particles were broken in the assembly.

Fig. 13 shows the comparison of the mass distribution of the particles at the end of compression for the experiments and simulation. It can be seen that the mass distribution

predicted by the simulations was similar to the experimental data. However, there is some noticeable difference in the mass percentage of particles in the <1.7 mm and 2.36-3.35 mm size ranges which shows some underestimation of breakage. This can be attributed to the following reasons:

(i) It can be seen in Fig. 12 that the top surface of the particle assembly is not level at the start of compression whereas in the experiments the surface was levelled before starting compression.

(ii) The smallest fragment size was set to 1 mm in order to ensure the simulation time would not become excessive because a smaller size would require a smaller time-step which would in turn increase simulation time.

(iii) The arrangement of particles in the assembly in the simulation is different than the experiment which affects the contact forces acting between the particles.

Conclusion

The focus of this study was to determine the strength distribution and breakage functions of mustard seeds, peppercorns, unrefined cane sugar and cake decorations by subjecting them to uniaxial compression. It was found that the mustard seeds do not fragment, while all the other materials tested do. A logistic function was fitted to the strength distribution of the materials and its empirical parameters were determined. The fragments formed from breakage of peppercorns, unrefined cane sugar and cake decoration particles were investigated to determine their breakage function. These functions were then implemented in DEM simulations to simulate single particle breakage and it was found that the simulations resulted in a qualitatively similar mass distribution of the daughter particles to the experiments. The BGU-DEM code was then applied to predict the simulation of bulk crushing of peppercorns. The mass distribution of the particles after compression in simulations appeared to be similar

to the experimental data however there was some underprediction of the fragments in the smallest size range.

Acknowledgement

This research is part of a PhD project funded by Glasgow Caledonian University. The authors would like to thank Dr. Andrew Cowell for his guidance in conducting the experiments, Stable Micro Systems Ltd. for providing the Texture Analyser and Prof. Avi Levy, Ben Gurion University, Israel, for providing the BGU-DEM code.

List of symbols

Symbol	Description	SI Units
a	Strength distribution function parameter	N
b	Strength distribution function parameter	-
c	Breakage function parameter	-
d_f	Size of the fragment	m
d_{max}	Size of the largest fragment	m
d_p	Size of the parent particle	m
k	Stiffness	$N/m^{1.5}$
m_f	Mass of the fragment	kg
m_{rel}	Relative mass	-
m_{norm}	Normalised mass	-
m_T	Total mass of fragments	kg
r	Particle radius	m
v	Relative velocity	m/s
B	Breakage function	-

C	Damping coefficient	Ns/m
E_p	Young's Modulus of particle	Pa
E_w	Young's Modulus of wall	Pa
F	Force	N
P	Breakage probability	-
V_f	Volume of fragment	m^3
V_p	Volume of parent particle	m^3
δ	Displacement	m
ρ	Particle density	kg/m^3
υ_p	Poisson's ratio of particle	-
υ_w	Poisson's ratio of wall	-

References

1. Brosh, T., and A. Levy. 2010. Modeling of heat transfer in pneumatic conveyer using a combined DEM-CFD numerical code. *Drying Technology* 28 (2): 155-164.
2. Brosh, T., H. Kalman, and A. Levy. 2011a. Fragments spawning and interaction models for DEM breakage simulation. *Granular Matter* 13 (6): 765-776.
3. Brosh, T., H. Kalman, and A. Levy. 2011b. DEM simulation of particle attrition in dilute-phase pneumatic conveying. *Granular Matter* 13 (2): 175-181.
4. Brosh, T., H. Kalman, A. Levy, I. Peyron, and F. Ricard. 2014. DEM–CFD simulation of particle comminution in jet-mill. *Powder Technology* 257 : 104-112.
5. Cleary, P. W., and M. D. Sinnott. 2015. Simulation of particle flows and breakage in crushers using DEM: Part 1 – compression crushers. *Minerals Engineering* 74 (0): 178-197.

6. Couroyer, C, Z Ning, and M Ghadiri. 2000. “Distinct Element Analysis of Bulk Crushing: Effect of Particle Properties and Loading Rate.” *Powder Technology* 109 (1–3): 241–54.
7. Kalman, H., V. Rodnianski, and M. Haim. 2009. A new method to implement comminution functions into DEM simulation of a size reduction system due to particle-wall collisions. *Granular Matter* 11 (4): 253-266.
8. Khanal, M., W. Schubert, and J. Tomas. 2005. “DEM Simulation of Diametrical Compression Test on Particle Compounds.” *Granular Matter* 7 (2): 83-90.
9. Pitchumani, R., O. Zhupanska, G. M. H. Meesters, and B. Scarlett. 2004. Measurement and characterization of particle strength using a new robotic compression tester. *Powder Technology* 143–144 (0): 56-64.
10. Rozenblat, Y., D. Portnikov, A. Levy, H. Kalman, S. Aman, and J. Tomas. 2011. Strength distribution of particles under compression. *Powder Technology* 208 (1): 215-224.
11. Subero-Couroyer, C., M. Ghadiri, N. Brunard, and F. Kolenda. 2003. Weibull analysis of quasi-static crushing strength of catalyst particles. *Chemical Engineering Research and Design* 81 (8): 953-962.
12. Vogel, L., and W. Peukert. 2002. Characterisation of grinding-relevant particle properties by inverting a population balance model. *Particle & Particle Systems Characterization* 19 (3): 149-157.
13. Wu, S. Z., K. T. Chau, and T. X. Yu. 2004. Crushing and fragmentation of brittle spheres under double impact test. *Powder Technology* 143–144 (0): 41-55.

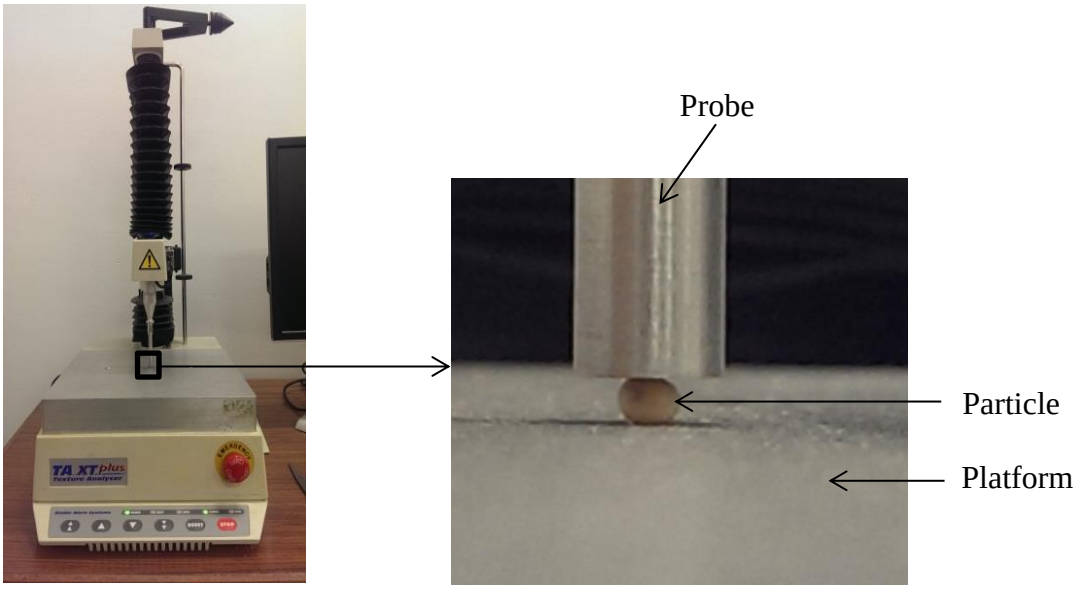

Fig. 1: TA XTPlus Texture Analyser

(a)

(b)

(c)

(d)

Fig. 2: (a) Mustard seeds (b) Peppercorns (c) Unrefined cane sugar (d) Cake decorations

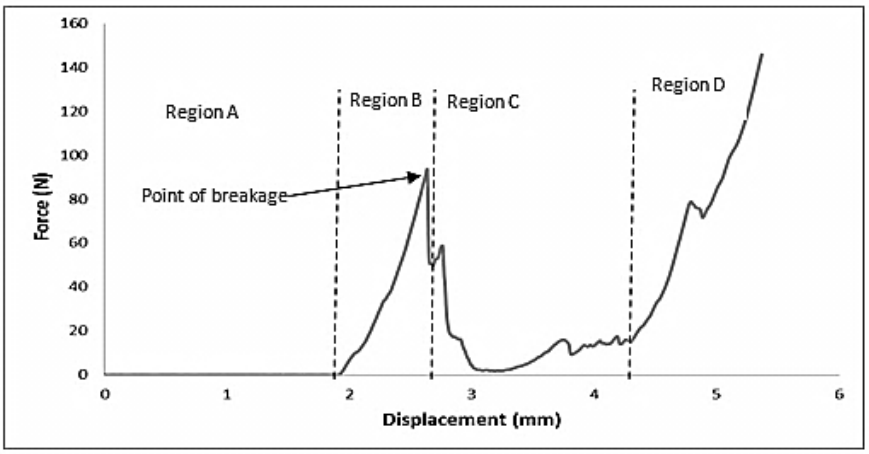

Fig. 3: Typical force vs displacement curve for a 4.14 mm peppercorn particle

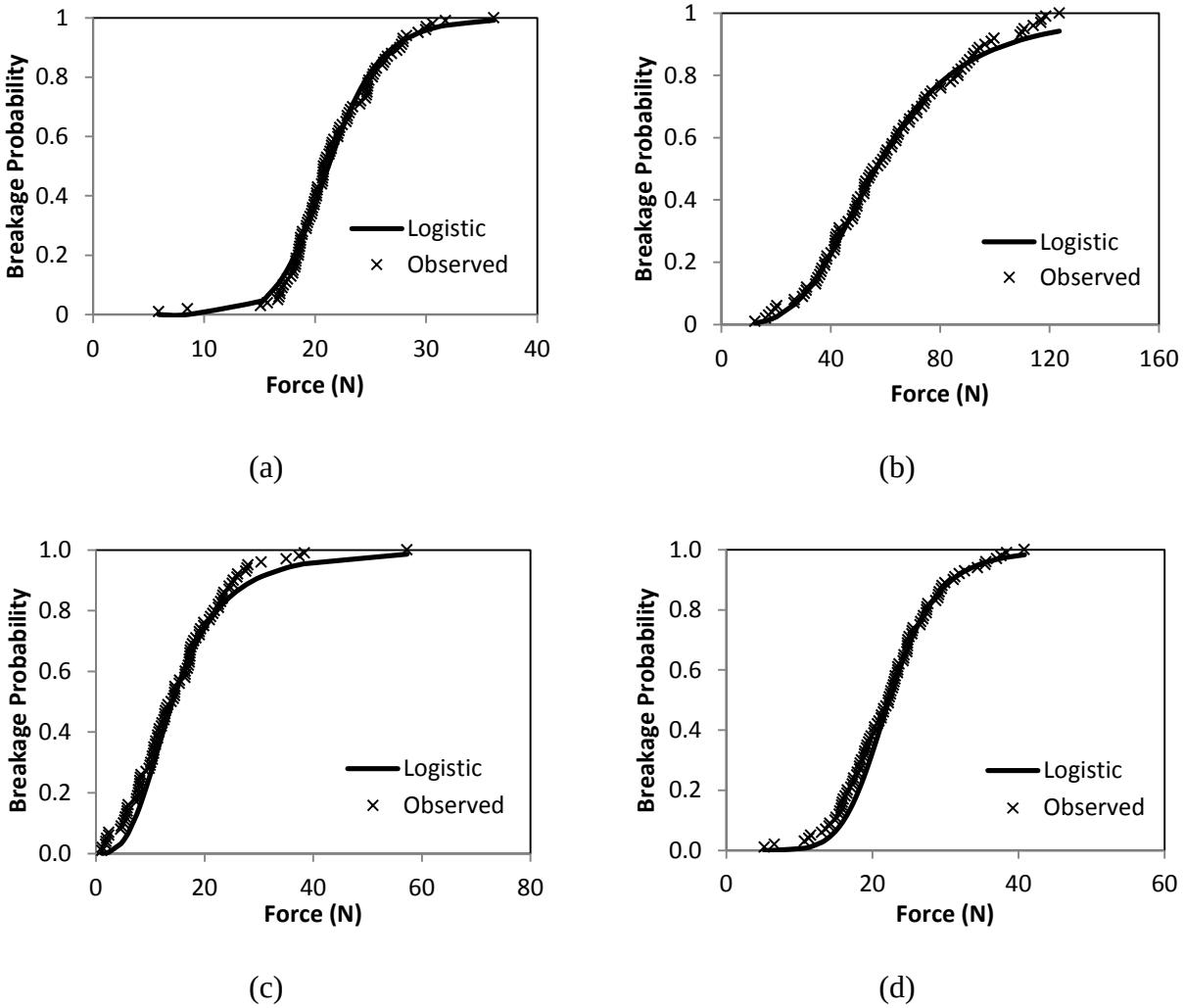

Fig. 4: Logistic function fit: (a) mustard seeds (b) peppercorns (c) unrefined cane sugar (d) cake decorations

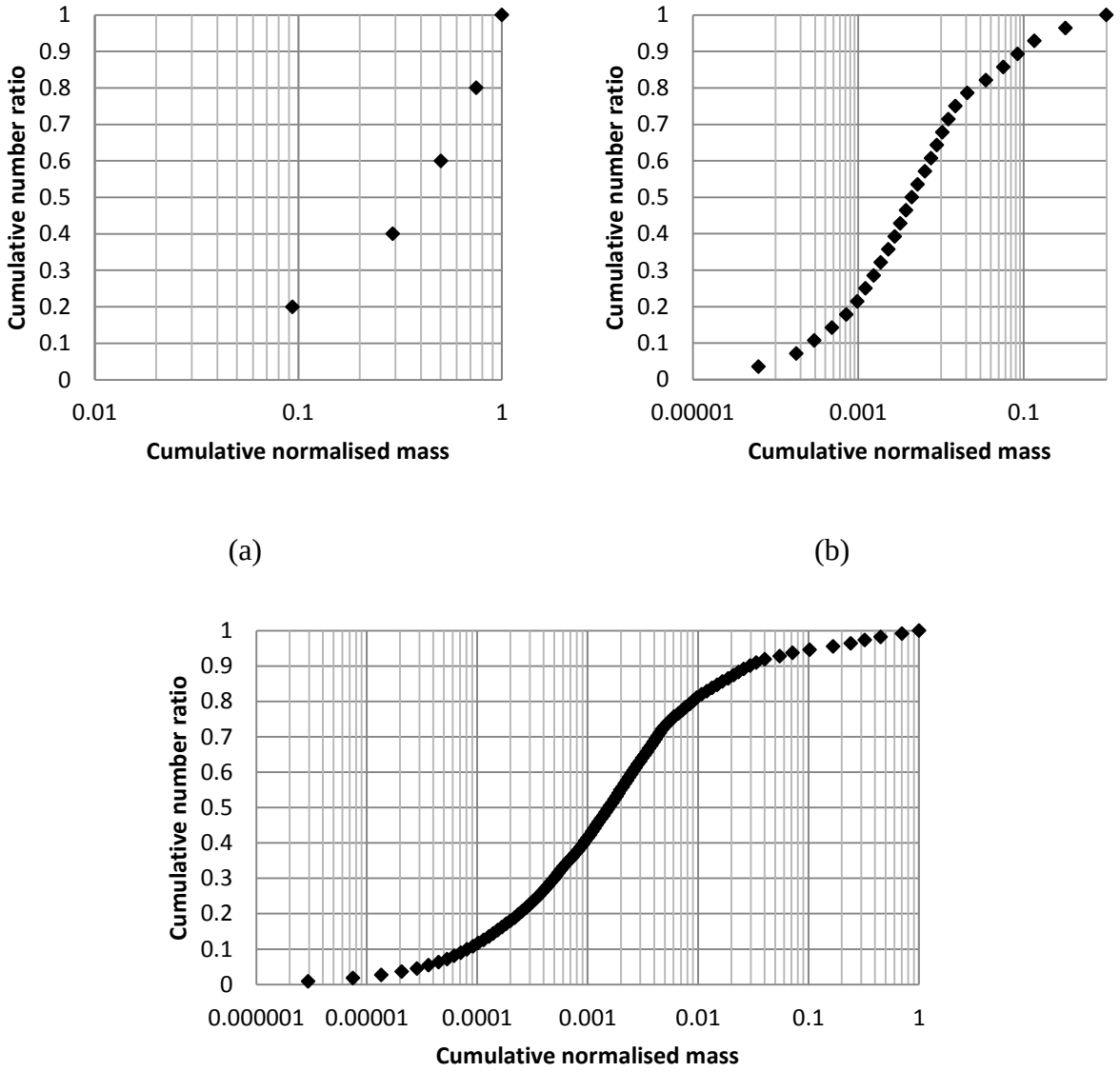

(a)

(b)

(c)

Fig. 5: Typical size distributions in terms of cumulative normalised mass (a) 4.3 mm peppercorn particle (b) 1.6 mm unrefined cane sugar particle (c) 2.02 mm cake decoration particle

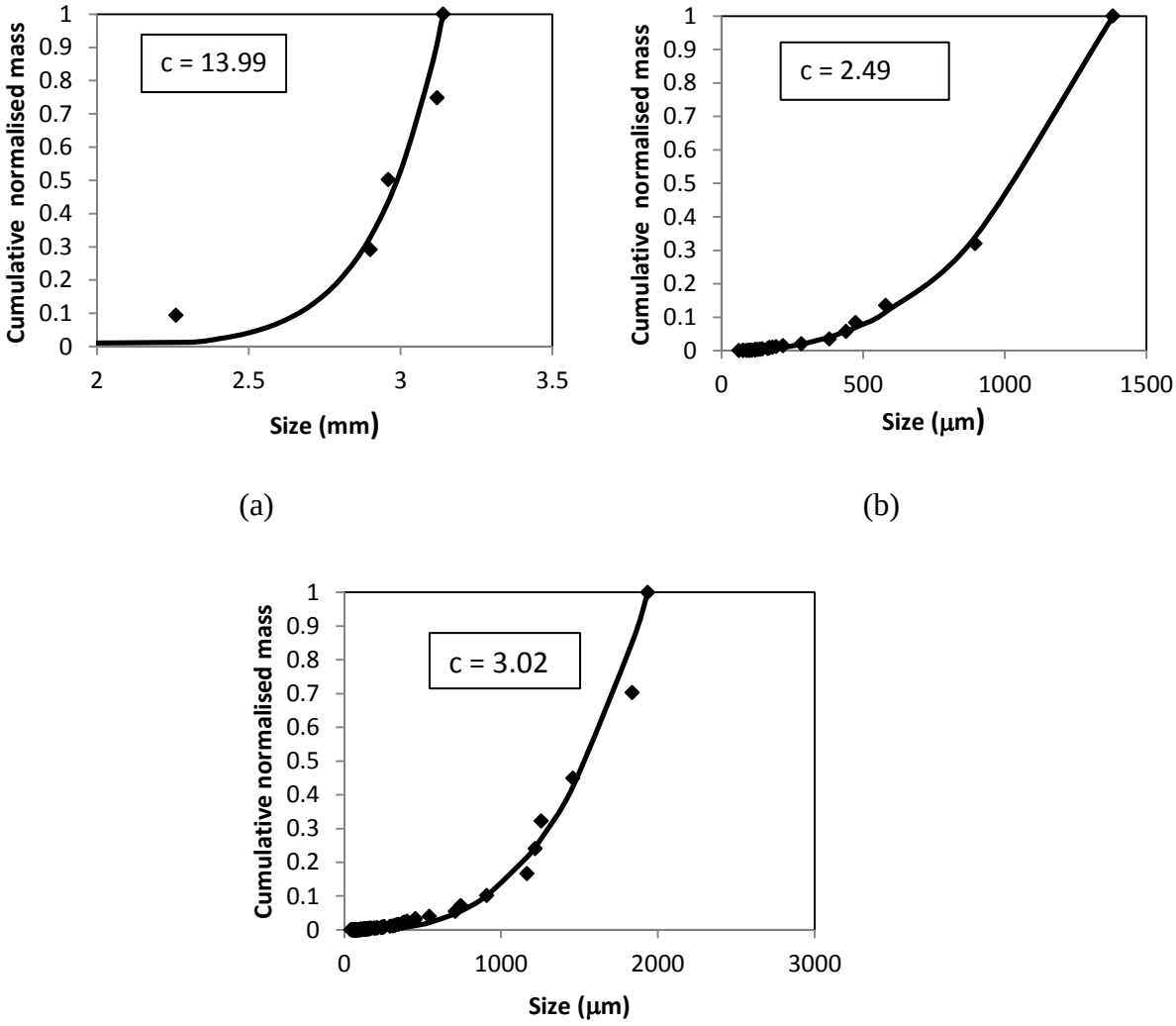

Fig. 6: Curve fitting of breakage function to normalised mass (a) 4.3 mm peppercorn particle (b) 1.6 mm unrefined cane sugar particle (c) 2.02 mm cake decoration particle. The solid line represents the breakage function and the points represent experimental data.

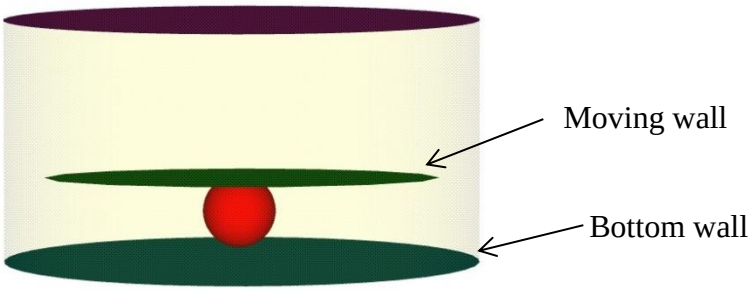

Fig. 7: Cylindrical domain with the particle placed on the bottom wall

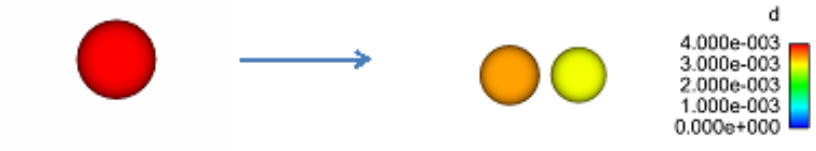

(a) Peppercorn particle

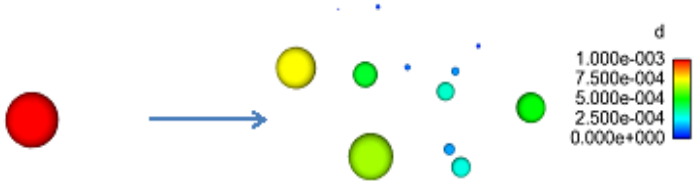

(b) Unrefined cane sugar particle

(c) Cake decoration particle

Fig. 8: Fragments formed after breakage in DEM simulations

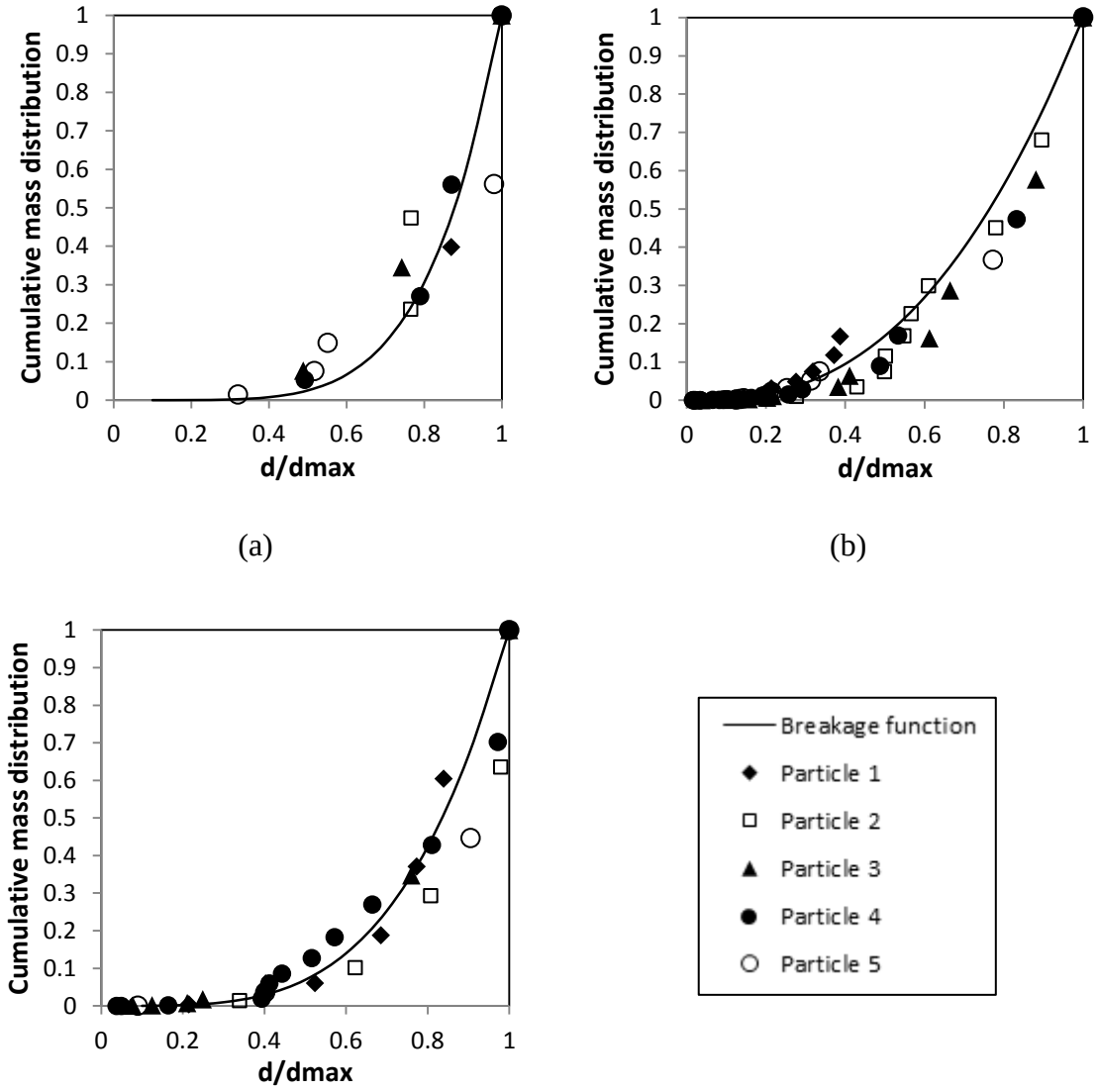

Fig. 9: Cumulative mass distribution after breakage in DEM simulations (a) peppercorns (b) unrefined cane sugar (c) cake decorations

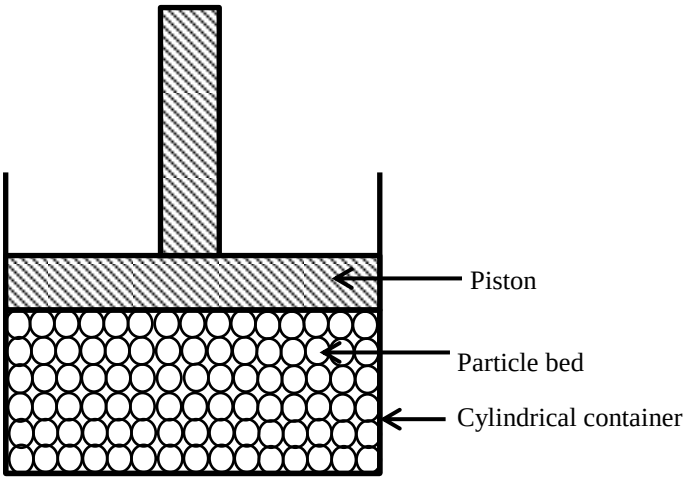

Fig. 10: Schematic of bulk crushing experiments (not to scale)

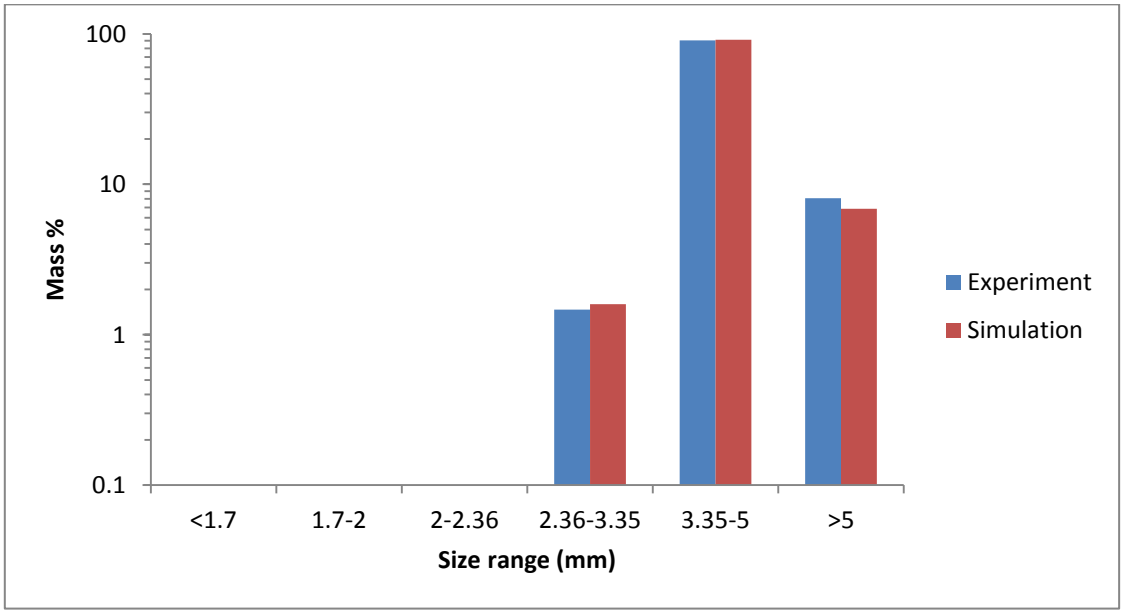

Fig. 11: Initial Size distribution of particles used in experiments and simulations

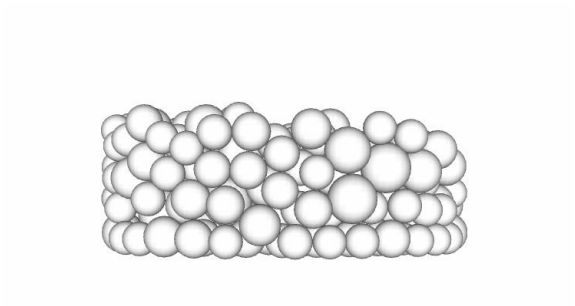

(a)

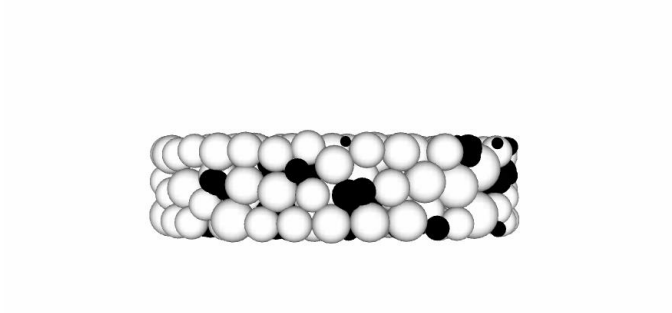

(b)

Fig. 12: Visualisation of particle assembly (a) before compression (b) after 5 mm compression

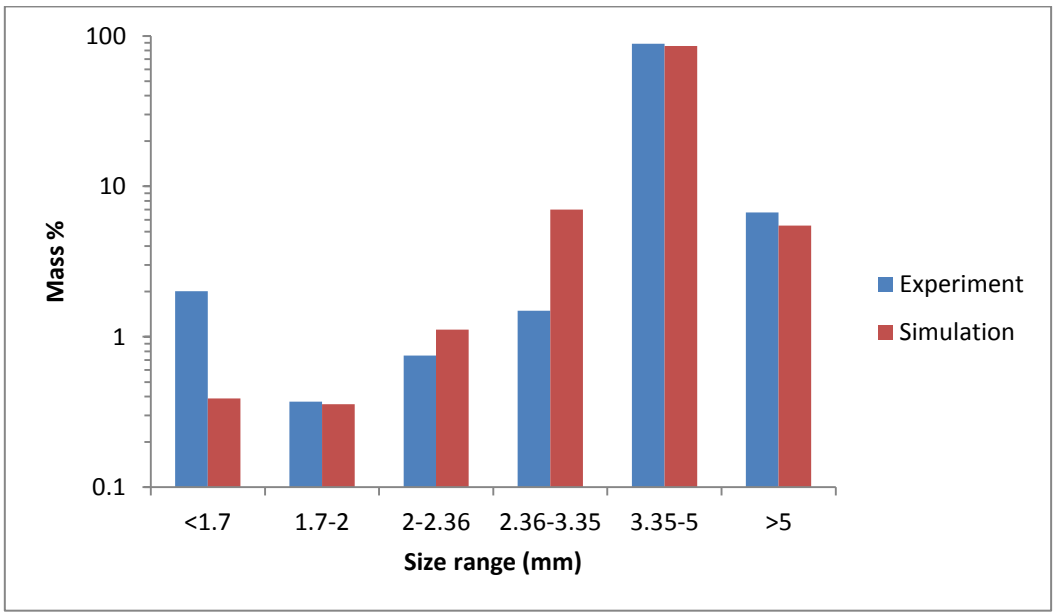

Fig. 13: Comparison of size distribution of particles after a compression of 5 mm in experiments and simulation

Table 1: Number of particles tested and statistical functions for strength distribution used by some previous researchers

Reference	No. of particles tested	Statistical function	Model	
Suber-Couroyer et al. (2003)	200	Weibull	$P = 1 - \exp\left[-\left(\frac{F}{a}\right)^{b}\right]$	(1)
Aman et al. (2010)	100	Lognormal	$P = \frac{1}{2}\left[1 + erf\left(\frac{\ln(F) - a}{b\sqrt{2}}\right)\right]$	(2)
Petukhov and Kalman (2004)	100	Logistic	$P = 1 - \frac{1}{1 + \left({}^{F}/_{a}\right)^{b}}$	(3)

Table 2: Materials

Material	Size (mm)
Mustard Seeds	1.6-2.6
Black peppercorns	3.4-5.4
Unrefined cane sugar	0.8-2.2
Cake decorations	1.2-2.0

Table 3: Summary of crushing force results

Force (N)	Mustard Seeds	Peppercorns	Unrefined cane sugar	Cake decorations
Maximum	36.11	123.56	57.25	40.82
Minimum	5.91	12.31	1.13	5.23
Mean	21.68	61.10	15.16	22.45
Median	20.83	56.45	14.09	22.29
Standard deviation	4.47	26.36	9.11	6.73

Table 4: Logistic function fitting summary

	Mustard Seeds	Peppercorns	Unrefined cane sugar	Cake decorations
a	21.19	56.44	13.42	21.77
b	8.99	3.57	2.75	5.71
R^2	0.9919	0.9962	0.9904	0.9971

Table 5: Parameter *c*

c	Peppercorns	Cake decorations	Cane sugar
Range	4.05-13.99	2.81-9.06	1.82-4.03
Mean	6.38	4.54	2.71

Table 6: Material and wall properties

	Young's modulus (GPa)	Poisson's ratio
Peppercorns	0.54	0.252
Unrefined cane sugar	4.99	0.252
Cake decorations	2.66	0.252
Wall	200	0.3